

Orlando P. Simonetti, PhD • J. Paul Finn, MD • Richard D. White, MD
Gerhard Laub, PhD • Daniel A. Henry, MD

“Black Blood” T2-weighted Inversion-Recovery MR Imaging of the Heart¹

PURPOSE: To develop a short-inversion-time inversion-recovery (STIR) magnetic resonance imaging pulse sequence for evaluating the myocardium that is relatively free of flow and motion artifact.

MATERIALS AND METHODS: The authors implemented a breath-hold, cardiac-triggered STIR sequence with preparatory radio-frequency pulses to eliminate signal from flowing blood. A segmented rapid acquisition with relaxation enhancement (turbo spin echo) readout was used, with the inversion-recovery delay adjusted to null fat. The sequence was implemented at 1.0 and 1.5 T and tested in phantoms, five healthy volunteers, and three patients.

RESULTS: Phantom studies confirmed the expected behavior of the sequence. In the volunteers, fat-suppressed images of the heart with STIR contrast were generated in a breath-hold period. Blood in the heart chambers was uniformly nulled, and motion artifacts were effectively suppressed. Focal high signal intensity consistent with edema was seen in two patients with acute myocardial infarction; in a third patient, a paracardiac mass was visualized and sharply demarcated relative to normal myocardium.

CONCLUSION: Fast STIR imaging of the heart with effective suppression of flow and motion artifact was implemented. The approach has much potential for high-contrast imaging in a variety of diseases affecting the heart and mediastinum.

Index terms: Heart, MR, 51.121413, 51.121415, 51.121416 • Magnetic resonance (MR), fat suppression • Magnetic resonance (MR), pulse sequences • Magnetic resonance (MR), rapid imaging • Myocardium, infarction, 511.771

Radiology 1996; 199:49-57

THE inherent sensitivity of magnetic resonance (MR) imaging to soft-tissue water is the basis of its success in detecting focal disease of the brain and musculoskeletal system. Changes in myocardial relaxation times have also been shown in a variety of pathologic conditions including infarction (1-5), tumors (5-7), infiltrative and deposition disease (5,8-10), and cardiac transplant rejection (5,11). However, implementation of MR imaging techniques capable of exploiting these changes has been frustrated by the combined effects of flow and physiologic motion artifact. In fact, the practical clinical applications of cardiac MR imaging have been effectively limited to morphologic and/or functional studies of the heart and imaging of the intracardiac blood pool (12).

The short-inversion-time inversion-recovery (STIR) technique (13) is sensitive to prolongation of both T1 and T2, which often coexist in disease states, and has proved superior to T2-weighted spin-echo (SE) sequences for many applications in musculoskeletal (13,14) and abdominal imaging (13,15). Sensitivity to changes in T1 and T2 and the homogeneous fat suppression possible with STIR offer theoretical advantages for imaging the myocardium. The potential of myocardial tissue characterization with conventional STIR has not been exploited, however, because of the severe artifacts caused by complex cardiac motion, respiratory motion, and pulsatile blood flow.

Segmented rapid acquisition with relaxation enhancement (RARE) (16), or turbo SE, techniques have recently been used for rapid T1-weighted

(17,18) and T2-weighted (19,20) imaging of the heart. Turbo SE offers the potential to create breath-hold, electrocardiogram (ECG)-triggered images of the heart that are essentially free of motion artifact. However, the relatively short repetition times (TRs) and long echo trains required to complete the sequence in a breath hold reduces the contrast in turbo SE imaging (21). Also, fat has high signal intensity on turbo SE images (21), which may be a source of confusion when a myocardial lesion is adjacent to epicardial fat. Combining a STIR preparation with the turbo SE technique (turbo STIR) suppresses fat signal and enhances the conspicuity of many types of focal lesions (22,23), while keeping imaging time to a reasonable breath-hold period. Unfortunately, conventional STIR and turbo STIR techniques are highly sensitive to flow artifact, severely limiting their effectiveness for detection of focal myocardial signal intensity changes.

To address the above limitations, we have developed a new pulse sequence for generating high-contrast turbo STIR images of the myocardium. The technique employs the strategies of breath holding, diastolic gating, and blood signal nulling to suppress the effects of respiration, cardiac motion, and pulsatile blood flow. Examples of such breath-hold images obtained in healthy volunteers and patients with myocardial disease are presented.

MATERIALS AND METHODS

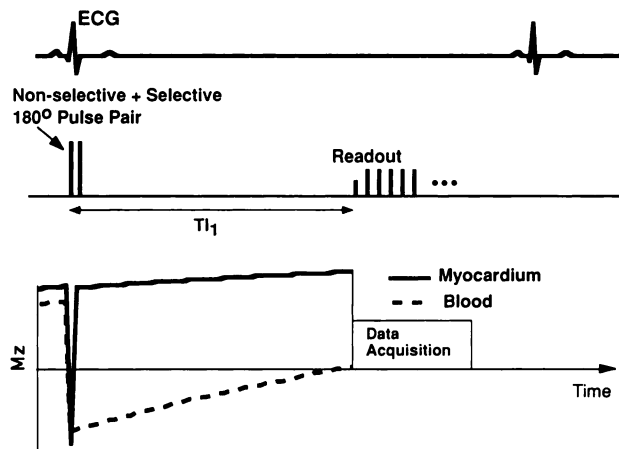
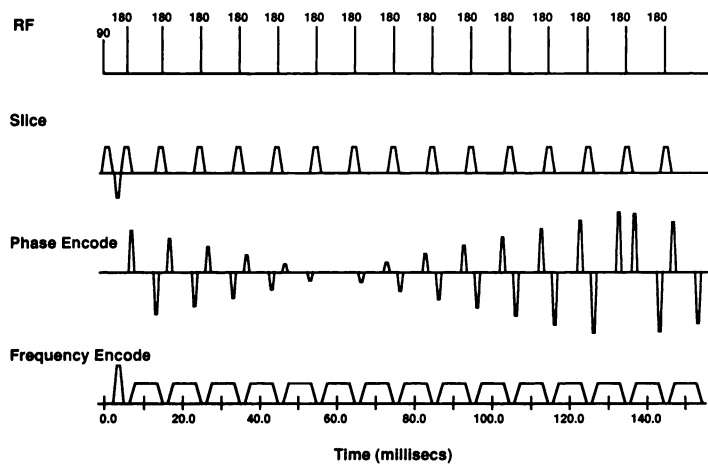
Pulse Sequence Design

The turbo STIR pulse sequence was designed as an extension of the turbo SE se-

¹ From MR Research and Development, Siemens Medical Systems, 186 Wood Ave S, Iselin, NJ 08830 (O.P.S., J.P.F.); Cleveland Clinic Foundation, Cleveland, Ohio (R.D.W.); Siemens AG, Erlangen, Germany (G.L.); and the Medical College of Virginia, Richmond (D.A.H.). From the 1994 RSNA scientific assembly. Received February 21, 1995; revision requested April 3; revision received October 13; accepted November 2. Address reprint requests to O.P.S.

• RSNA, 1996

Abbreviations: AMI = acute myocardial infarction, ECG = electrocardiogram, SE = spin echo, STIR = short-inversion-time inversion recovery, TE = echo time, T₁ = long inversion time, T₂ = short inversion time, TR = repetition time.



Figures 1, 2. (1) Basic turbo SE acquisition module. Fifteen SEs are acquired for each 90° pulse. The phase-encoding gradient pulses are ordered so as to acquire the central lines of k-space with the sixth echo, for an effective echo time (TE) of 61 msec. The echo spacing is 10.24 msec, and the sampling bandwidth is 195 Hz per pixel. RF = radio frequency. (2) Timing diagram shows the effect of the blood nulling preparatory pulses. The T1 recovery curves are shown for myocardium and out-of-section blood. Nonselective inversion applied at the R wave of the ECG is followed immediately by a section-selective inversion pulse. The net result of this pulse pair is inversion of all spins (tissue and blood) outside the imaged section plane. Image acquisition is timed to occur as the longitudinal magnetization of blood recovers through the null point, which suppresses blood signal.

quence illustrated in Figure 1. An echo train length of 15 echoes with an interecho spacing of 10.24 msec and a sampling bandwidth of 195 Hz per pixel were used. To minimize sensitivity to cardiac motion, the echo train duration was kept below 160 msec, while still permitting image acquisition in a breath hold of 16–20 heartbeats. A TR of two RR intervals was typically used. A longer TR may be desirable to minimize T1 weighting and maximize signal but would result in an unacceptable breath-hold duration. For example, in 16 heartbeats, a 120 × 256 image can be acquired during suspended respiration in a segmented fashion by sampling 15 phase-encoding steps (“lines”) every second heartbeat. The sixth of 15 echoes was used to encode the center of k-space, yielding an effective TE of 61 msec.

The scheme used for attenuating blood signal was originally described for segmented gradient-echo imaging (24,25). A spatially nonselective 180° pulse is followed immediately by a section-selective 180° pulse (Fig 2). The net effect is to invert all spins outside the image section, while spins within the section experience both 180° prepulses and therefore undergo zero net nutation. Blood flowing into the section plane during the long inversion time (TI₁) is affected only by the nonselective inversion; TI₁ is chosen close to the null point of blood, typically about 600 msec in the above implementation at normal heart rates.

Serendipitously, the periodic events of the cardiac cycle make this technique of blood signal suppression effective in cardiac imaging. As shown in Figure 3, the nonselective 180° plus the section-selective 180° pulse pair is applied immediately after the R-wave trigger, while the heart is in its relaxed, end-diastolic state. Systole follows, and most of the blood within the selected section that has experienced both

Table 1
Null Point of Blood for Different TRs

Heart Rate (bpm)	RR (msec)	TR (msec)*	Null Point of Blood (msec)
100	600	1,200	400
80	750	1,500	530
60	1,000	2,000	625

* TR = 2 × RR.

inversions is washed out of the section. The heart then returns to its end-diastolic position, and the image data are acquired. Since the acquisition does not occur at exactly the same point in the cardiac cycle as the preparation pulses, a band of selective inversion with a thickness two times that of the imaged section is used to allow for some misregistration of tissue within the inversion band. This also allows for imperfections in the inversion section profile. At an RR interval of 1,000 msec (TR of 2,000 msec), the null point of blood (T₁ = 1,200 msec at 1.5 T) occurs at approximately 625 msec; this varies with TR, as described by Fleckenstein et al (26) and as indicated in Figure 4. The longitudinal magnetization of blood does not relax fully from the previous excitation by the end of the typical TR period. Thus, the magnetization available for subsequent inversion is less than if relaxation were complete, and the null point is achieved more quickly than in the case of an infinite TR. Table 1 lists the null point of blood for different TRs and indicates that blood signal can be successfully suppressed with this technique over a wide range of heart rates. The technique relies on washout of blood during systole

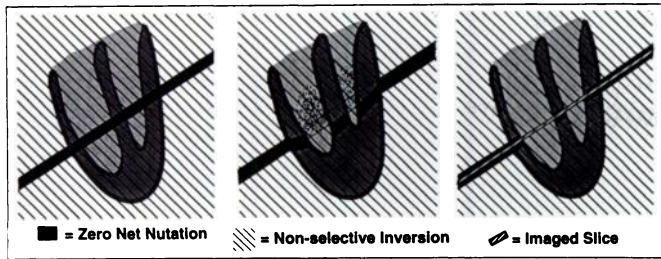
Table 2
T1 and T2 Values for Solutions in the Multicompartment Phantom

Solution No.	T1 (msec)	T2 (msec)
1	85	50
2	307	251
3	606	63
4	783	83
5	885	125
6	1,365	168
7	1,766	235

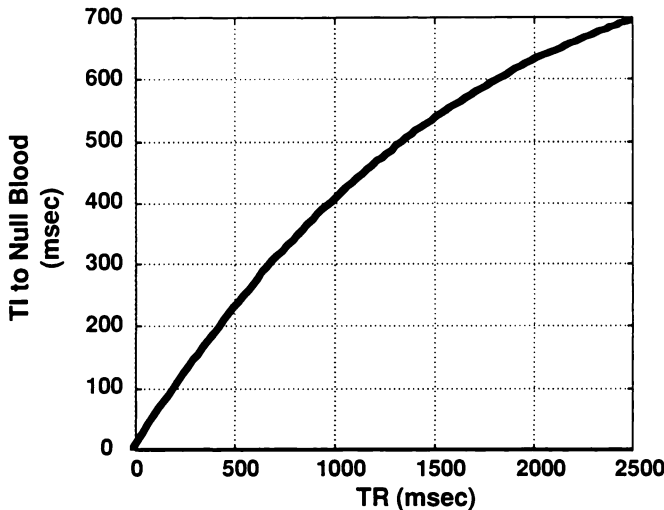
Note.—Solution numbers correspond to those in Figure 7b.

and may not be completely effective if the flow is slow or mainly in plane.

The “black blood” turbo SE sequence shown in Figure 2 is converted to a black blood turbo STIR sequence with the addition of a section-selective inversion pulse (Fig 5). The STIR pulse is applied approximately 150 msec before the 90° excitation pulse, with the same turbo SE readout module shown in Figure 1. The short inversion time (TI₂) has two effects: Fat is suppressed because of its short T₁, and T₁ and T₂ relaxation processes add constructively. Tissues with long T₁ and T₂ have relatively high signal intensity due to the combination of inverse T₁ weighting with the short-inversion preparation and T₂ weighting with the relatively long TE. The effects of the STIR preparation pulse on fat, blood, and normal myocardium, when used with the double-inversion blood suppression preparation, were modeled mathematically and are diagrammed in Figure 5. STIR works best in combination with the blood inversion, provided that it is applied near—ideally after—the null point of blood. If the blood magnetization has



3.

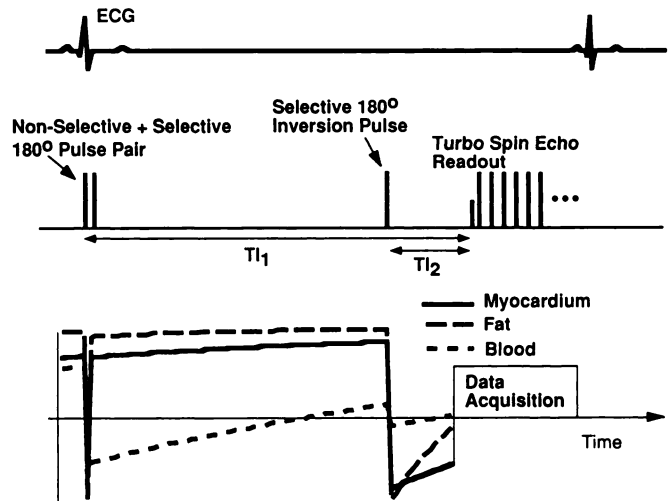


4.

not yet reached its null, the next inversion pulse will drive the signal toward its positive equilibrium value. In Figure 5, the blood is assumed to remain within the section plane after the STIR inversion, since it is applied in mid-to-late diastole, and the time between the inversion and excitation pulses is relatively short (approximately 150 msec). In practice, it is not crucial to hit the null point of the blood signal exactly, since the T1 relaxation of blood is relatively slow and effective suppression can be achieved over a wide range of inversion times.

Phantom Measurements

Blood-suppression preparation pulse.—A uniform spherical nickel chloride-doped water phantom was imaged to examine the effectiveness and section profile of the double-inversion blood nulling preparation pulses. The T1 of the phantom was approximately 300 msec. For purposes of illustration, the inversion pulses were applied orthogonal to the imaged section. In this manner, the effectiveness of out-of-section inversion and the resulting section profile could be examined directly. A turbo SE sequence without a STIR inversion pulse was used. The inversion time (TI₁) was set to 200 msec to approximately null the phantom solution. The section thickness for the selective inversion pulse was set at 16 mm. Both the selective and non-selective inversion pulses used the same 10.24-msec hyperbolic secant radio-frequency envelope (27). This relatively long-



5.

Figures 3–5. (3) Illustration of the timing and events of nonselective plus selective inversion blood suppression preparation within the cardiac cycle. Events of the cardiac cycle work in concert with the double-inversion preparation. The inversion pulse pair is applied at end diastole. The inversion time extends over systole, allowing uninverted blood to wash out of the section plane before data acquisition. The 90° excitation pulse is then applied after the heart has returned to its diastolic position. (4) The inversion time (TI) to null blood varies as a function of TR, as described by Fleckenstein et al (26). This is fortuitous in cardiac applications because a diastolic image with blood signal suppression can be obtained over a wide range of heart rates. (5) Timing diagram shows the combined effects of the blood nulling and STIR preparatory pulses. The longitudinal magnetization of in-plane fat, myocardium, and out-of-section blood are simulated. Blood is assumed to remain within the image plane during the second inversion time (TI₂). TI₁ nulls blood signal, while TI₂ serves to enhance contrast between long T1 and short T1 tissues.

duration pulse provides good B₁ insensitivity and inversion section profiles.

Contrast and fat suppression.—A multi-compartment phantom with five different solutions of manganese chloride, one nickel chloride solution, and a bottle of mineral oil were imaged to compare the contrast obtained with the turbo STIR sequence (with and without the blood nulling preparation) with a conventional SE STIR sequence. TE was set at 61 msec and TR at 2,000 msec for both the conventional SE and turbo STIR sequences. Average signal intensity measurements were calculated for the six phantom solutions and mineral oil to examine the effects on contrast of using a turbo SE readout and the blood nulling preparation. Predetermined T1 and T2 values for these solutions are listed in Table 2.

Subjects and Imaging Methods

Human studies were initially performed in five healthy volunteers to optimize pulse sequence parameters. Informed consent was obtained before all studies. Normalized liver-spleen contrast-to-noise ratio was computed as $(S_{\text{spleen}} - S_{\text{liver}}) / (S_{\text{spleen}} + S_{\text{liver}}) / \sigma_{\text{noise}}$ where S is the mean signal and σ is the standard deviation of background noise. This was done to evaluate the combined relaxation time weighting of the turbo STIR technique. Liver-spleen contrast-to-noise ratio is accepted as a use-

ful figure of merit for imaging the liver and was used in the present study because no reference standards are defined for normal myocardial T2 contrast. Additionally, long- and short-axis turbo SE and turbo STIR images of healthy subjects were qualitatively analyzed by two independent observers (J.P.F., O.P.S.) for the presence of motion and flow artifacts according to the following scale: 0 = none, 1 = minimal, 2 = moderate, and 3 = severe.

To develop insights into the potential clinical applications of these techniques, three adult patients with heart disease were studied with the approval of the institutional Investigational Review Boards, and informed consent was obtained in all cases. Two patients were examined within a week after acute myocardial infarction (AMI), to determine if the turbo STIR sequence can depict changes due to myocardial edema.

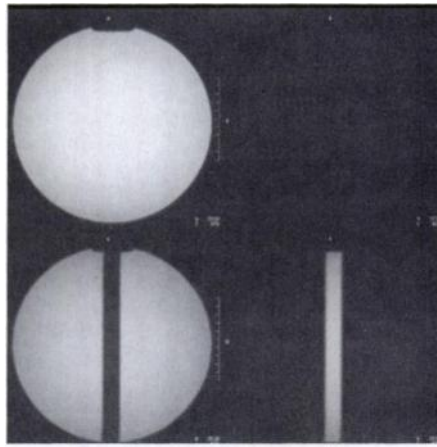
The first patient was a 73-year-old woman with a documented transmural anterior AMI, confirmed by means of 12-lead ECG (Q waves in precordial leads V₁–V₄ associated with ST-segment elevation) and cardiac enzyme profiles (markedly elevated creatine kinase values, to > 1,500 U/L with a > 4% MB enzyme fraction). Coronary angiography on the day of presentation revealed more than 90% narrowing of the proximal left anterior descending coronary artery with occlusive thrombus distally. No clinically significant

disease was seen in the right coronary or left circumflex coronary arteries. The patient successfully underwent thrombolytic therapy with intravenous tissue plasminogen activator and emergency percutaneous transluminal coronary angioplasty of the proximal left anterior descending coronary artery lesion (28). Resting multigated radionuclide blood-pool ventriculography on day 4 showed a depressed ejection fraction of 44% with anteroseptal and anteroapical wall motion abnormalities (29). MR imaging was performed on the same day.

The second AMI patient was a 42-year-old man with a documented transmural posteroinferior infarct, confirmed by means of standard ECG (Q waves in frontal leads II, III, and aVF) and cardiac enzyme profiles (markedly elevated creatine kinase values, to > 2,000 U/L with a > 4% MB enzyme fraction, and reversal of the lactate dehydrogenase fractions). On the day of the acute event, this patient underwent thrombolytic therapy with intravenous streptokinase infusion (28). Thallium-201 stress SPECT (single photon emission computed tomography) perfusion scanning performed on day 5 showed an irreversible defect in the inferoposterior and posterolateral regions, and echocardiography on day 6 showed segmental wall motion abnormalities in the posterior and lateral regions (29). MR imaging was initially performed in this patient on day 5. The same patient underwent repeat MR imaging with the turbo SE and turbo STIR techniques on day 47 after the acute event. In the interval, the patient was pain free, treated medically, and not subjected to any further diagnostic or interventional procedures.

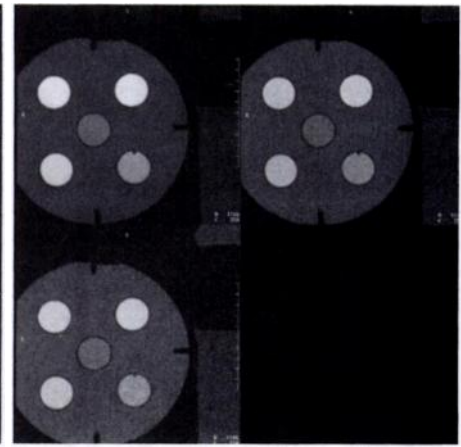
The third patient was a 43-year-old woman who had a paracardiac mass that was discovered incidentally during work-up for unrelated symptoms. After chest radiography showed an abnormality, thoracic computed tomography revealed a large soft-tissue mass contiguous with the posterior wall of the left ventricle. Attempted biopsy resulted in profuse bleeding at thoracotomy, and the procedure was abandoned, with a presumptive (but unproved) diagnosis of hemangioma. Serial cardiac MR imaging studies with T1-weighted conventional and turbo SE sequences (18) demonstrated a slightly lobulated 6 × 6-cm mass contiguous with the left ventricular free wall. The signal intensity of the mass was only slightly different from that of myocardium, and the boundary between the tumor and the left ventricular myocardium was poorly defined. Because surgical excision of the mass was judged to be a high-risk procedure, a conservative approach to treatment was adopted. MR imaging with breath-hold T2-weighted turbo SE and turbo STIR was requested to better define the boundaries of the mass for possible future surgical intervention.

All images were acquired with standard commercial MR imagers (Magnetom Vision and Impact; Siemens Medical Systems, Iselin, NJ). Phantom, volunteer, and all but one of the patient studies were obtained with a 1.5-T Vision system equipped

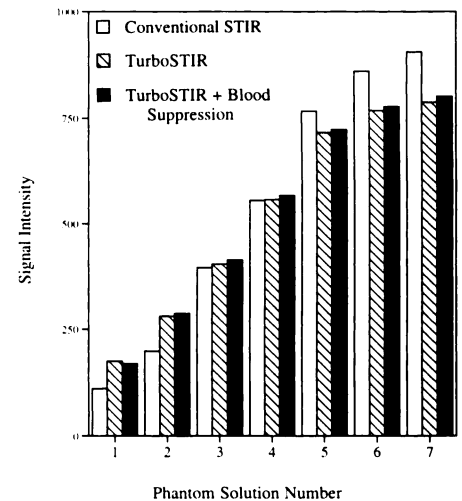
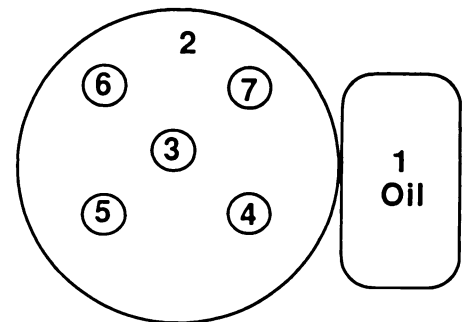


6.

Figures 6, 7. (6) MR images of a uniform spherical phantom demonstrate the out-of-section inversion preparation. The preparatory pulses are applied orthogonal to the imaged section for demonstration purposes. Images were acquired without preparatory pulses (top left), with a nonselective inversion pulse with the inversion time set at 200 msec to null the phantom solution (top right), with a 10.24-msec hyperbolic secant section-selective inversion pulse (bottom left), and with the combined selective-nonselective preparation showing the net effect of out-of-section nulling (bottom right). The signal in the prepared section is approximately 95% of the original signal. (7a) MR images of a multicompartiment phantom demonstrate similar contrast characteristics with conventional STIR (top left, TR msec/TE msec = 2,000/61), turbo STIR (top right, TE = 61 msec), and turbo STIR with the blood nulling preparatory pulses (bottom left, TE = 61 msec). Some degradation of contrast is expected with turbo STIR relative to conventional STIR because of inclusion of short TE echoes in the image data. (7b) Schematic (top) of the phantom. Numbers correspond to those in Table 2 (which lists the relaxation parameters of the phantom compartments). Bar graph (bottom) of signal intensities with different imaging techniques shows slight degradation of contrast and a reduction in signal-to-noise ratio with a turbo STIR readout relative to conventional STIR; however, the double-inversion blood nulling preparation has little effect on contrast.



7a.



7b.

with 25 mT/m gradient hardware. The patient with the cardiac mass was studied with a 1.0-T Impact system equipped with 15 mT/m gradient hardware. A standard body coil was used routinely, with the subjects positioned supine. The field of view in the phase-encoding direction was user definable and was chosen to maximize spatial resolution within a given breath-hold period.

In addition to breath-hold turbo STIR, patients were examined with breath-hold T2-weighted turbo SE sequences and, where appropriate, cine MR imaging of the heart. For the breath-hold STIR and T2-weighted studies, TR was set to twice the RR interval and the inversion time (T_1) for blood signal suppression was set to the maximum allowed by the subject's

RR interval. The STIR inversion time (T_2) was set to 150 msec at 1.5 T and 130 msec at 1.0 T. Typical section dimensions were an 8-mm thickness, a 300 × 400-mm rectangular field of view, and a 120 × 256 data matrix, giving an in-plane resolution of 2.5 × 1.6 mm.

Sections were acquired in multiple orientations, including axial, coronal, and long- and short-axis double-oblique planes. The entire span of the myocardium could be interrogated in eight to 10 sections per plane. Tagged cine (30,31) MR images were acquired in one patient to qualitatively examine myocardial wall motion. In this technique, a grid of saturation bands is applied at the R-wave trigger, followed by acquisition of gradient-echo

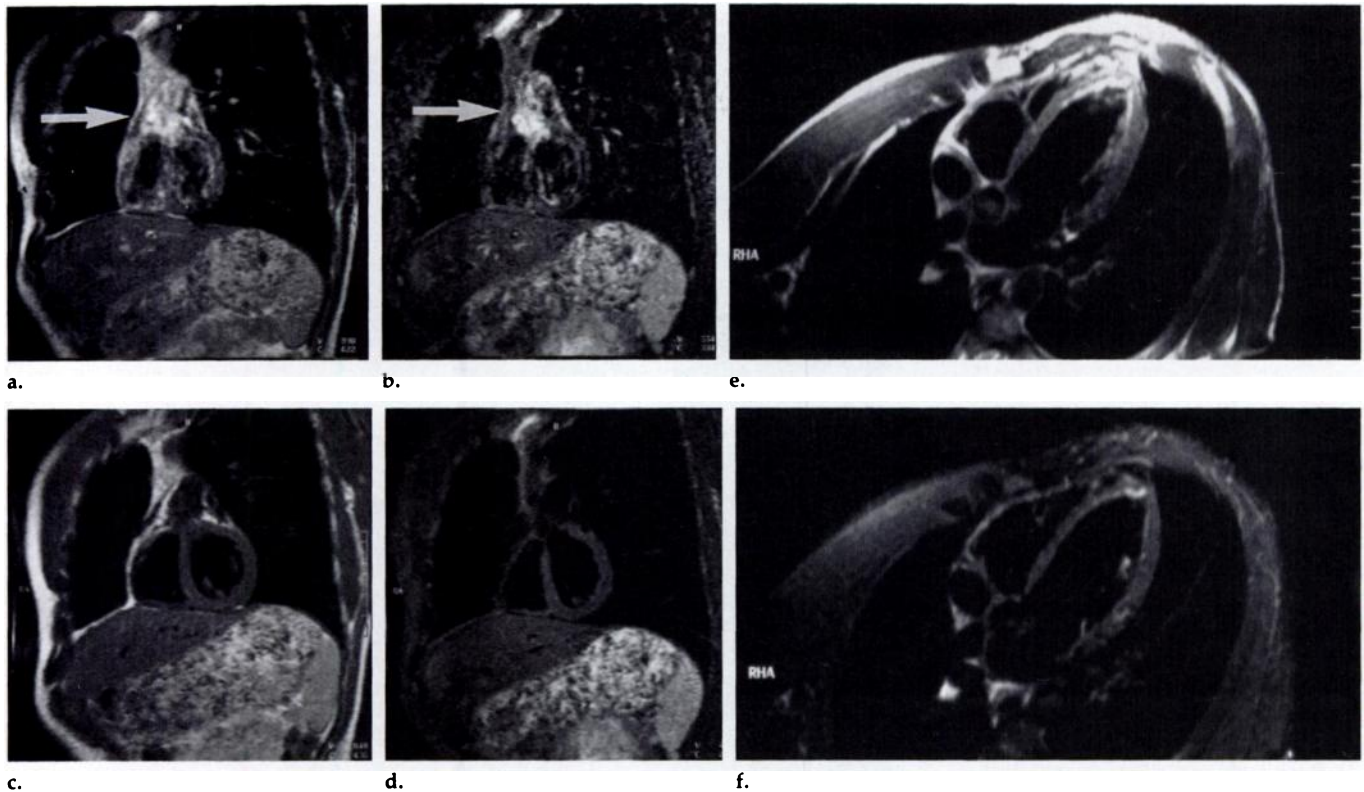


Figure 8. (a–d) Breath-hold, ECG-triggered MR images in a healthy volunteer demonstrate the effect of the blood nulling and STIR preparations. Oblique coronal images were obtained with (a) turbo SE without any preparatory pulses (TE, 93 msec), (b) turbo STIR without blood nulling (TE, 61 msec), (c) turbo SE with blood nulling (TE, 93 msec), and (d) turbo STIR with blood nulling (TE, 61 msec). Note the severe artifacts caused by slow flow and in-plane flow when the blood nulling preparation is not used (arrow in a and b). (e, f) Long-axis images in a second volunteer acquired with (e) turbo SE (TE, 93 msec) and (f) turbo STIR (TE, 61 msec) show that some high-signal-intensity blood remains along the inner wall of the left ventricle near the apex, due to insufficient through-plane flow in this orientation.

cine images. The saturation grid provides visual landmarks within the myocardium that can reveal deficiencies in regional cardiac wall motion. The tagged cine images were acquired with the following parameters: 285 × 380-mm field of view, 128 × 256 image matrix, 8-mm section thickness, TR of 40 msec, TE of 7 msec, 16 frames per cardiac cycle, flip angle of 30°, and three signals averaged. Binomial pulses were used to generate a saturation tag grid with 8-mm spacing between the tag lines.

RESULTS

Phantoms

The images shown in Figure 6 demonstrate the effects of the blood nulling preparatory pulse pair. Uniform nulling of the phantom signal outside the double-inversion section is evident. Comparison of the signal in the double-inversion section to that in the image with no preparatory pulses reveals that 95% of the signal intensity is preserved. The thickness of the double-inversion section matches that of the single-inversion section.

The images in Figure 7a and the signal intensities in the graph in Figure 7b illustrate how the contrast obtained with the turbo STIR sequence

with and without the blood nulling preparation compares with that of the conventional STIR sequence. While the same contrast trend is observed with all three sequences, the contrast is slightly flatter with turbo STIR than with conventional STIR imaging. The blood nulling preparation causes no further degradation of contrast.

Volunteers

Images of two healthy volunteers are shown in Figure 8. Figure 8a and 8b indicate the importance of blood signal suppression. Figure 8a was acquired without the blood nulling preparation or STIR. Note the high-signal-intensity fat characteristic of the turbo SE sequence and the artifacts caused by blood in the cardiac chambers and ascending aorta. In Figure 8b, STIR was applied but no blood nulling preparation was used. Flow artifacts severely degrade the image. Figure 8c and 8d illustrate the success of the double-inversion preparation in eliminating blood flow artifacts. Blood is uniformly nulled within the cardiac chambers and the aorta, and fat is uniformly suppressed on the turbo STIR image.

Figure 8e and 8f are long-axis black blood turbo SE and turbo STIR images, respectively, of a second volunteer. Note some remaining high-intensity blood signal along the inner wall of the left ventricle near the apex. This is due to insufficient through-plane flow for the blood nulling preparation to be completely effective. Some slight flow artifact is evident in the lateral wall of the left ventricle, also due to incomplete suppression of blood signal within the heart.

In the five volunteers and three patients examined, the liver-spleen contrast-to-noise ratio was significantly higher ($P < .025$) on the turbo STIR images than on the T2-weighted turbo SE images.

The results of qualitative analysis of images for artifact are summarized in Table 3. The average grade (in the range 0–3) for each observer is listed in each of the categories.

Patients

Myocardial and mediastinal images of good quality were obtained in all patients, and no patients had difficulty with breath holding. In the pa-

Table 3
Results of Qualitative Analysis of Motion and Flow Artifacts in Volunteers

Observer	T2-weighted Turbo SE Images		Turbo STIR Images	
	Short Axis	Long Axis	Short Axis	Long Axis
1	0.25	0.75	0.5	1.25
2	0.25	0.75	0.75	1.25

Note.—Data are average grades (grade range, 0–3).

tient with the septal infarct, the turbo STIR sequence revealed a generalized increase in myocardial signal intensity in the interventricular septum and the adjacent anterior and anteroapical regions of the left ventricular wall (Fig 9). This was interpreted as edema and corresponded to marked hypokinesia on cine MR images and tagged wall motion studies (30,31) (Fig 9d).

In the second AMI patient, the turbo STIR sequence on day 5 after the acute event showed focal hyperintensity within the subendocardial and epicardial layers of the posterolateral and posteroinferior left ventricle, interpreted as edema. Within the middle myocardial layer, lower signal intensity was observed and was interpreted as local post-reperfusion hemorrhage (32) (Fig 10a, 10b). Follow-up MR imaging on day 47 revealed normalization of signal intensity and pronounced myocardial thinning in the region of the infarct (Fig 10c, 10d).

In the patient with the mass lesion, T2-weighted turbo SE (Fig 11b) and turbo STIR (Fig 11c) images showed high contrast between tumor and ventricular muscle and defined the interface between the mass and myocardium better than T1-weighted images. The marked T2 hyperintensity of the lesion was interpreted as consistent with that of a vascular tumor. Follow-up studies have shown no change in the size or shape of the mass, and the patient remains symptom free.

DISCUSSION

The results of this study indicate that black blood turbo STIR generates images of the myocardium that are highly sensitive to changes in tissue relaxation times and that have minimum flow and motion artifacts. Previous research has demonstrated that changes in T1 and T2 accompany a

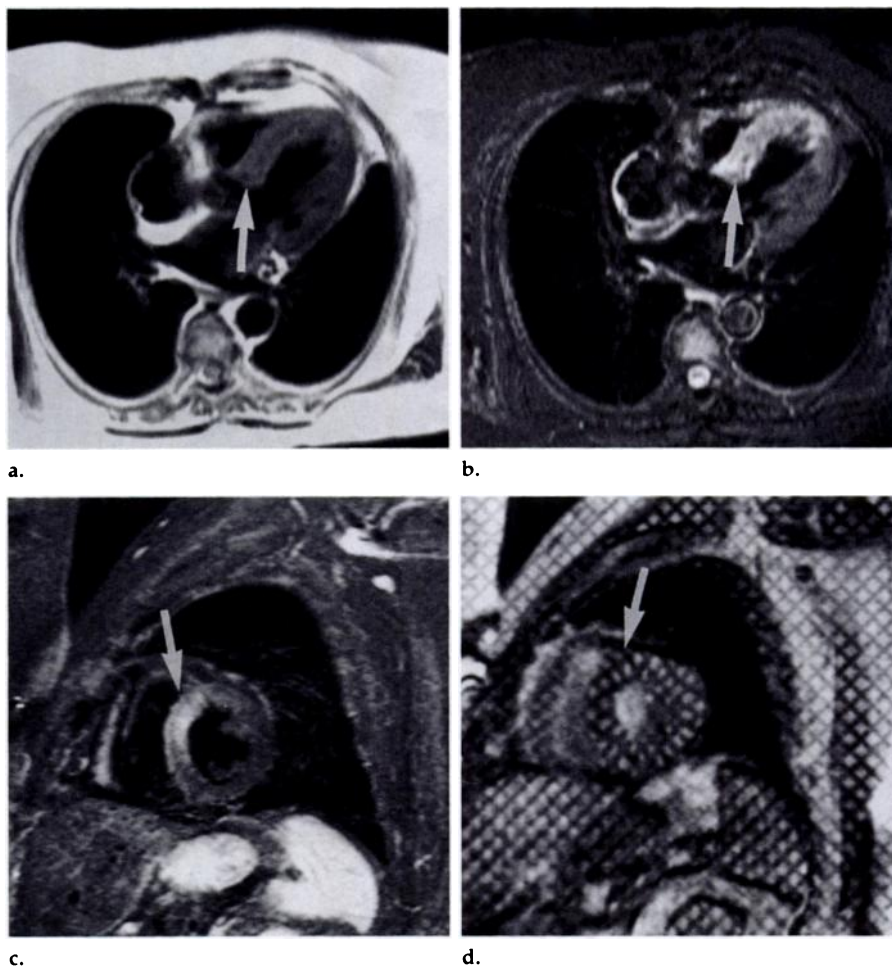


Figure 9. Septal myocardial infarction, 4 days after AMI. (a, b) Transverse T2-weighted (a) turbo SE (TE, 93 msec) and (b) turbo STIR (TE, 61 msec) images. An increase in signal intensity in the interventricular septum (arrow) extending anteriorly is evident on both images and was interpreted as representing edema. The turbo STIR image demonstrates the benefits of fat suppression and increased contrast compared with the T2-weighted image. The normalized contrast-to-noise ratio (see text) between edematous and normal myocardium was approximately twice as high in the turbo STIR image than the T2-weighted turbo SE image (0.034 vs 0.016). Short-axis (c) turbo STIR (TE, 61 msec) and (d) tagged gradient-echo cine images show correspondence between the septal signal intensity change (arrow in c) on the turbo STIR image and the relative hypokinesia in the same region (arrow in d) on the tagged image.

wide variety of myocardial diseases, including myocardial infarction (1–11). MR imaging should, in principle, be a powerful modality for noninvasive diagnosis of pathologic changes in heart muscle. This has not been the case because of the severity of motion artifacts in T2-weighted and conventional STIR imaging of the heart, the techniques most sensitive to changes in tissue relaxation times.

In the present study, several steps were taken to avoid or eliminate sources of motion artifact. To eliminate respiratory motion, the acquisition time was reduced to a reasonable breath-hold period by acquiring 15 lines of data in a cardiac cycle. The trade-offs in turbo SE imaging are well known. The drastic reduction in acquisition time necessarily results in some reduction in signal-to-noise ra-

tio, as shown in the phantom studies (Fig 7); however, in practice, this was more than offset by the elimination of respiratory artifacts. Contrast is also modified by the inclusion of data from a wide range of TEs, as shown in Figure 7. Image contrast with turbo SE techniques is determined mainly by the TE used to encode the low spatial frequencies. In the present study, positioning the sixth echo at the center of k-space provided moderate T2 weighting in the turbo STIR images while maintaining a reasonable signal-to-noise ratio with the body coil.

Techniques that rely on breath holding are most successful in stable and cooperative patients. It is, of course, desirable to keep breath-hold periods to a minimum. Recent advances in gradient hardware and surface coil design have been used both

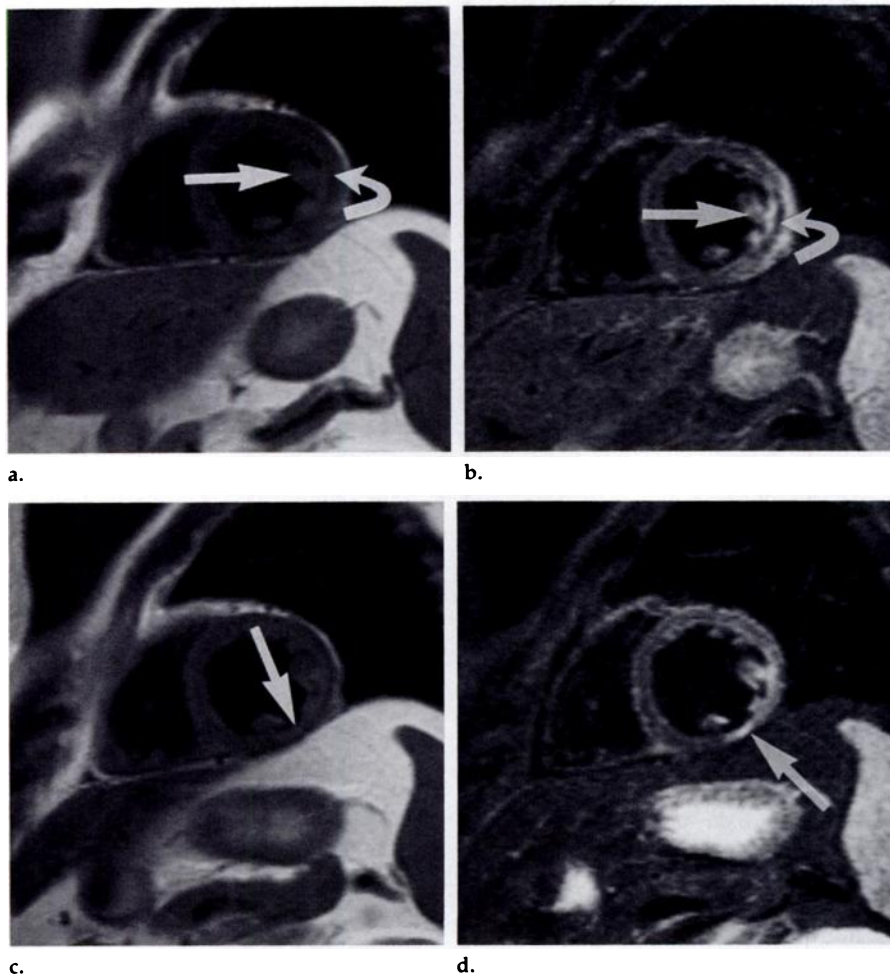


Figure 10. Posterolateral myocardial infarction (a, b) 5 and (c, d) 47 days after the acute event. Focal signal hyperintensity is evident in the posterolateral wall, extending into the anterolateral papillary muscle (straight arrow in a and b), on both the (a) turbo SE (TE, 93 msec) and (b) turbo STIR (TE, 61 msec) images and was interpreted as representing edema. Also evident is a linear low-signal-intensity region within the wall (curved arrow in a and b), interpreted as post-reperfusion hemorrhage. The normalized contrast-to-noise ratio (see text) between edematous and normal myocardium was approximately twice as high on the turbo STIR image than the T2-weighted turbo SE image (0.031 vs 0.016). (c, d) At follow-up examination, short-axis (c) T2-weighted turbo SE (TE, 93 msec) and (d) turbo STIR (TE, 61 msec) images show pronounced thinning in the posterolateral wall (arrow).

to increase the number of lines acquired per cardiac cycle and decrease the total number of lines required by reducing the field of view. The combined effect should be a substantial reduction in breath-hold time and may provide the capability of imaging more than one section per breath-hold period.

Diastolic imaging is a requirement of the blood signal suppression technique. The diagram in Figure 3 indicates that out-of-section inversion blood nulling can work only if the preparatory pulses and image acquisition both take place when the myocardium is in the same position. Otherwise, myocardium that has experienced only the nonselective inversion will be imaged. Nonselective inversion has been used in black blood cardiac imaging at low field

strength, in which the T1 values of blood and myocardium are further separated (33). However, at high field strength, the T1 of myocardium (850 msec at 1.5 T) is nearly as long as that of blood, and its signal would be attenuated if a nonselective inversion preparation were used to suppress blood signal. Loss of myocardial signal, primarily in the free wall, was one source of artifact noted on the volunteer images by the two observers. In practice, this signal loss can be largely prevented by timing the image acquisition to late diastole when the myocardium has nearly recovered to its end-diastolic position.

The profile and relative thickness of the band of selective reinversion is important to the success of the out-of-section inversion technique. Some excess thickness is required as a safety

margin to accommodate possible misregistration of tissue between the preparation and the readout modules. The trade-off in using a wider inversion profile is that more blood is reinverted and a higher through-plane velocity is required for complete washout. In practice, we found that a thickness two times that of the imaged section provides a good balance between these effects. A thicker reinversion zone can be used in the short-axis view, in which most of the flow is through plane. Thinner reinversion should be used in long-axis or four-chamber views, in which both flow and myocardial motion are primarily in plane. Not all the blood from the cardiac chambers is replaced with each cardiac cycle, and some magnetized blood remains as a source of potential signal, as seen in the long-axis images of the volunteers. The increased artifacts in long-axis views noted by the two observers was primarily due to residual blood signal. In low-ejection-fraction states, this may become a more important factor; however, this effect was not important in the patient studies shown.

Another important factor in choosing the thickness of the reinversion slab is the profile of the inverted sections. When multiple inversion pulses are used sequentially, imperfections in section profiles are propagated. The hyperbolic secant pulse envelope used in the present study (27) provides complete inversion, insensitivity to B_1 inhomogeneity, and excellent section profiles, as shown in the phantom images in Figure 6.

When triggering to every second R wave, the timing and events of the cardiac cycle work in concert with the blood nulling preparation over a wide range of heart rates (Table 1). In ECG-triggered acquisitions, the TR is an integer multiple of the RR interval; TRs are shorter at faster heart rates, and less time is available within the RR interval for a long inversion delay. Fortunately, the inversion time (TI_1) to null blood also decreases with TR, because the blood does not return to its full equilibrium state. The blood nulling preparation, therefore, works well over a wide range of heart rates. In practice, the inversion time (TI_1) is chosen to place the acquisition as late in diastole as possible, rather than to hit the null point of blood exactly. Extending TI_1 within the cardiac cycle allows maximum washout of in-plane blood between the preparatory pulses at the R wave and the 90° excitation pulse for the turbo SE acquisition. Pushing the acquisition window to

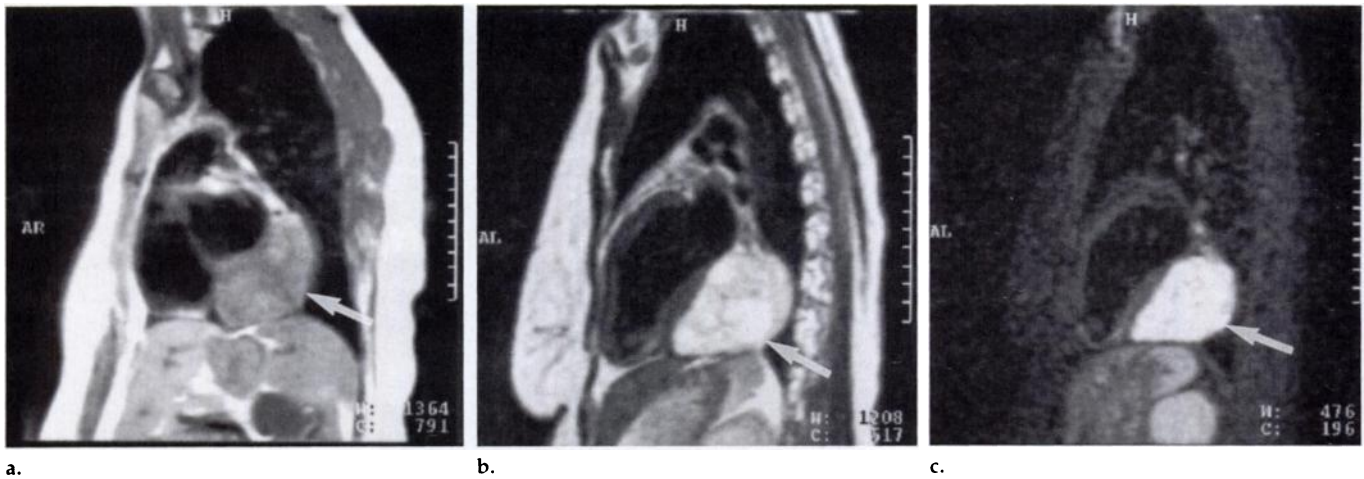


Figure 11. Oblique (a) T1-weighted turbo SE (TE, 35 msec), (b) T2-weighted turbo SE (TE, 93 msec), and (c) turbo STIR (TE, 61 msec) images of a large mass (arrow) attached to the left ventricular free wall and interpreted as a hemangioma. The high signal intensity of the mass clearly delineates it from the myocardium on the T2-weighted turbo SE and turbo STIR images.

late diastole also allows the myocardium to return to its end-diastolic position. The 90° selective-excitation pulse is thus applied to the same section of myocardium that experienced both 180° inversion pulses at the R-wave trigger. Myocardial motion throughout the cardiac cycle then does not lead to misregistration between the prepared and imaged sections. Also, given the relatively long T1 of blood, changes in the longitudinal magnetization occur slowly, so the inversion time can be offset somewhat from the exact null point while still achieving effective blood signal suppression. The familiar SE effects of washout and dephasing also contribute to blood signal suppression, as shown in the volunteer images without the double-inversion preparation (Fig 8).

The motivation for designing this technique was to make the contrast advantages of STIR available in cardiac imaging. T2 weighting can be compromised somewhat in turbo SE imaging because of the inclusion of short TE echoes in the raw data matrix. The STIR T₁ inversion pulse serves to null the signal from very short T1 tissues, such as fat, and to generate additive T1 and T2 contrast, causing fluid and tissues with high water content to appear bright, similar to the contrast on a heavily T2-weighted image. In principle, STIR should be sensitive to myocardial tissue changes in a variety of diseases, provided that motion artifacts are controlled. The phantom images in Figure 7 indicate that contrast holds up well when the STIR pulse is combined with a multiline turbo SE readout and the blood nulling preparation pulses. This is demonstrated in the

volunteer and patient images as well (Figs 8–11).

The preliminary clinical results presented in this report clearly show the potential advantages of the turbo STIR technique. The results in AMI patients were encouraging (Figs 9, 10). Focal signal intensity changes were shown more dramatically, from the standpoint of definition and brightness, than is typically achieved with traditional MR imaging, even with the use of contrast agents. For some time, relaxation time changes have been known to accompany infarction and may potentially be used for discriminating reperfusion, hemorrhage, healing, and scarring. To our knowledge, this potential has not been exploited to date, mainly because of the poor image quality and long acquisition times associated with T2-weighted SE imaging of the heart.

In conclusion, this report describes a technique for MR imaging of the heart and adjacent mediastinal regions that overcomes problems with cardiac and respiratory motion by means of rapid imaging, blood signal suppression, and breath holding. Preliminary clinical results show promise that breath-held, black blood turbo STIR imaging may be sensitive to the focal changes of myocardial infarction or edema and, together with established methods, may help characterize the nature and extent of myocardial injury. Formal clinical evaluation of the technique is necessary to define its ultimate role in cardiac imaging. ■

References

- Higgins CB, Herfkens R, Lipton MJ, et al. Nuclear magnetic resonance imaging of acute myocardial infarction in dogs: alterations in magnetic relaxation times. *Am J Cardiol* 1983; 52:184–188.
- Wesbey G, Higgins CB, Lanzer P, Botvinick E, Lipton MJ. Imaging and characterization of acute myocardial infarction in vivo by gated nuclear magnetic resonance. *Circulation* 1984; 69:125–130.
- Been M, Smith MA, Ridgeway JP, et al. Serial changes in the T1 magnetic relaxation parameter after myocardial infarction in man. *Br Heart J* 1988; 59:1–8.
- Johnston DL, Homma S, Liu P, et al. Serial changes in nuclear magnetic resonance relaxation times after myocardial infarction in the rabbit: relationship to water content, severity of ischemia, and histopathology over a six-month period. *Magn Reson Med* 1988; 8:363–379.
- Johnston DL. Myocardial tissue characterization with magnetic resonance imaging techniques. *Am J Cardiac Imaging* 1994; 8:140–150.
- Winkler M, Higgins CB. Suspected intracardiac masses: evaluation with MR imaging. *Radiology* 1987; 165:117–122.
- Lund JT, Ehman RL, Julsrud PR, Sinak LJ, Tajik AJ. Cardiac masses: assessment by MR imaging. *AJR* 1989; 152:469–473.
- Levine RA, Weyman AE, Dinsmore RE, et al. Noninvasive tissue characterization: diagnosis of lipomatous hypertrophy of the atrial septum by nuclear magnetic resonance imaging. *J Am Coll Cardiol* 1986; 7:688–692.
- Scholz TD, Fleagle SR, Parrish, FC, Breon T, Skorton DJ. Effect of tissue fat and water content on nuclear magnetic resonance relaxation times of cardiac and skeletal muscle. *Magn Reson Imaging* 1990; 8:605–611.
- Blake LM, Scheinman MM, Higgins CB. MR features of arrhythmogenic right ventricular dysplasia. *AJR* 1994; 162:809–812.
- Wisenberg G, Pflugfelder PW, Kostuk WJ, et al. Diagnostic applicability of magnetic resonance imaging in assessing human allograft rejection. *Am J Cardiol* 1987; 60:130–136.
- White RW, Ehman RL, Weinreb JC. Cardiovascular MR imaging: current level of clinical activity. *JMRI* 1992; 2:365–370.
- Bydder GM, Young IR. MR imaging: clinical use of the inversion recovery sequence. *J Comput Assist Tomogr* 1985; 9:659–675.
- Dwyer AJ, Frank JA, Sank VJ, et al. Short-TI inversion recovery pulse sequence: analysis and initial experience in cancer imaging. *Radiology* 1988; 168:827–836.

15. Bydder GM, Steiner RE, Blumgart LH, Khenia S, Young IR. MR imaging of the liver using short TI inversion recovery sequences. *J Comput Assist Tomogr* 1985; 9:1084-1089.
16. Hennig J, Nauwerth A, Friedburg H. RARE imaging: a fast imaging method for clinical MR. *Magn Reson Med* 1986; 3:823-833.
17. Liu Y, Riederer SJ, Ehman RL, Rydberg J. Breath-hold cardiac imaging using fast spin-echo and short TR gradient echo techniques (abstr). In: *Book of abstracts: Society of Magnetic Resonance in Medicine 1992*. Berkeley, Calif: Society of Magnetic Resonance in Medicine, 1992; 2528.
18. Simonetti OP, Kiefer B, Laub G, Fluegel H, Finn P. Rapid black-blood imaging of the heart with turbo spin-echo and turbo gradient spin-echo techniques (abstr). *JMRI* 1994; 4(P):81.
19. Seelos KC, von Smekal A, Vahlensieck M, Gieseke J, Reiser M. Cardiac abnormalities: assessment with T2-weighted turbo spin-echo MR imaging with electrocardiogram gating at 0.5 T. *Radiology* 1993; 189: 517-522.
20. Simonetti OP, Laub G, Finn P. Breath-hold T2-weighted imaging of the heart with turbo spin-echo (abstr). In: *Proceedings of the Society of Magnetic Resonance 1994*. Berkeley, Calif: Society of Magnetic Resonance, 1994; 1499.
21. Constable RT, Anderson AW, Zhong J, Gore JC. Factors influencing contrast in fast spin-echo MR imaging. *Magn Reson Imaging* 1992; 10:497-511.
22. Smith RC, Constable RT, Reinhold C, et al. Inversion-recovery fast spin-echo MR imaging (abstr). *Radiology* 1991; 181(P):202.
23. Panush D, Fulbright R, Sze G, Smith RC, Constable RT. Inversion-recovery fast spin-echo MR imaging: efficacy in the evaluation of head and neck lesions. *Radiology* 1993; 187:421-426.
24. Edelman RR, Chien D, Kim D. Fast selective black blood MR imaging. *Radiology* 1991; 181:655-660.
25. Liu Y, Riederer SJ, Ehman RL. Magnetization-prepared cardiac imaging using gradient echo acquisition. *Magn Reson Med* 1993; 30:271-275.
26. Fleckenstein JL, Archer BT, Barker BA, Vaughan JT, Parkey RW, Peshock RM. Fast short-tau inversion-recovery MR imaging. *Radiology* 1991; 179:499-504.
27. Silver MS, Joseph RI, Hoult DI. Highly selective p/2 and p pulse generation. *J Magn Reson* 1984; 59:347-351.
28. Braunwald E. The aggressive treatment of acute myocardial infarction. *Circulation* 1985; 71:1087-1091.
29. Pasternak RC, Braunwald E, Sobel BE. Acute myocardial infarction. In: Braunwald E, ed. *Heart disease: a textbook of cardiovascular medicine*. 4th ed. Philadelphia, Pa: Saunders, 1992; 1200-1291.
30. Zerhouni EA, Parish DM, Rogers WJ, Yang A, Shapiro EP. Human heart tagging with MR imaging: a method for noninvasive assessment of myocardial motion. *Radiology* 1988; 169:59-63.
31. Axel L, Dougherty L. MR imaging of motion with spatial modulation of magnetization. *Radiology* 1989; 171:841-845.
32. Weisfeldt ML. Reperfusion and reperfusion injury. *Clin Res* 1987; 35:13-19.
33. Mayo JR, Culham JAC, MacKay AL, Aikins DG. Blood MR signal suppression by pre-excitation with inverting pulses. *Radiology* 1989; 173:269-271.